

- ¹¹S. Margulies and J. R. Ehrman, Nucl. Instr. Methods **12**, 131 (1961).
- ¹²L. D. Roberts, D. O. Patterson, J. O. Thomson, and R. P. Levey, Phys. Rev. **179**, 656 (1969).
- ¹³D. O. Patterson, J. O. Thomson, P. G. Huray, and L. D. Roberts, Phys. Rev. B **2**, 2440 (1970).
- ¹⁴M. Bresesti and J. C. Roy, Can. J. Chem. **38**, 194 (1960).
- ¹⁵D. Nagle, P. P. Craig, J. G. Dash, and R. R. Reiswig, Phys. Rev. Letters **4**, 237 (1960).
- ¹⁶H. J. Andrä, C. M. H. Hashmi, P. Kienle, and F. W. Stanek, Z. Naturforsch. **18A**, 687 (1963).
- ¹⁷L. D. Roberts and J. O. Thomson, Phys. Rev. **129**, 664 (1963).
- ¹⁸R. W. Ohlweiler, dissertation, University of California, Davis, 1968 (unpublished).
- ¹⁹J. W. Mihelich and A. de-Shalit, Phys. Rev. **91**, 78 (1953).
- ²⁰D. A. Shirley, M. Kaplan, and P. Axel, Phys. Rev. **123**, 816 (1961).
- ²¹R. S. Hager and E. C. Seltzer, Nucl. Data **A4**, (1968).
- ²²I. J. van Heerden, D. Reitmann, and H. Schneider, Nuovo Cimento **11**, 167 (1959).
- ²³B. Jung and J. Svedberg, Arkiv Fysik **19**, 429 (1961).
- ²⁴A. Bäcklin and S. G. Malmkog, Arkiv Fysik **34**, 59 (1967).
- ²⁵O. Huber, J. Halter, R. Joly, D. Maeder, and J. Brunner, Helv. Phys. Acta **26**, 591 (1953); R. Joly, J. Brunner, J. Halter, and O. Huber, *ibid.* **28**, 403 (1955).
- ²⁶C. Günther (private communication).
- ²⁷O. Dragoun, Z. Plajner, and F. Schmutzler (unpublished); we are indebted to O. Dragoun (private communication) for generously supplying us with the appropriate ICC's for $Z=79$ and $E_\gamma=77.3$ keV from these tables prior to publication.
- ²⁸E. F. Skelton and J. L. Feldman (unpublished).
- ²⁹J. C. Manthuruthil and J. H. Hamilton, in Proceedings of the International Conference on Radioactivity in Nuclear Spectroscopy, Vanderbilt University, Nashville, Tenn., 1969 (unpublished).
- ³⁰J. R. Harris, N. Benczer-Koller, and G. M. Rothberg, Phys. Rev. **137**, A1101, (1965).
- ³¹J. L. Feldman and G. K. Horton, Phys. Rev. **137**, A1106 (1965).
- ³²J. R. Harris, G. M. Rothberg, and N. Benczer-Koller, Phys. Rev. **138**, B554 (1965).
- ³³J. Speth and F. W. Stanek, Z. Naturforsch. **20A**, 1175 (1965).
- ³⁴J. W. Marshall and R. M. Wilenzick, Phys. Rev. Letters **16**, 219 (1966).
- ³⁵D. L. Martin, Phys. Rev. **170**, 650 (1968).
- ³⁶T. H. Geballe and W. F. Giaque, J. Am. Chem. Soc. **74**, 2368 (1952).
- ³⁷The different averages over a frequency distribution which determine the recoilless fraction and the lattice specific heat are discussed by R. H. Nussbaum, in *Mössbauer Effect Methodology*, edited by I. J. Gruverman (Plenum, New York, 1966), Vol. II, p. 3.
- ³⁸G. E. Shoemaker and J. A. Rayne, Phys. Letters **26A**, 222 (1968).

Electronic Structure and Spectrum of the NiF_6^{4-} Cluster: Results of Calculations Based on Self-Consistent-Field Models*

Thomas F. Soules,[†] James W. Richardson, and David M. Vaught[‡]

Department of Chemistry, Purdue University, Lafayette, Indiana 47907

(Received 24 August 1970)

Restricted and unrestricted Hartree-Fock molecular-orbital self-consistent-field calculations were performed on the cluster NiF_6^{4-} with a fixed internuclear distance appropriate to KNiF_3 . A slightly extended multicenter atomic-orbital basis was used. In contrast to the approach of earlier calculations which sought to describe $10Dq$ as a single electron promotion between t_{2g} and e_g antibonding (LCAO) molecular orbitals, we obtained the spectra as the difference in energy between various many-electron open-shell states. The results obtained with limited configuration interaction are in good agreement with the five observed optical absorption bands. We find that the earlier orbital picture can be approximately maintained only if the covalency parameters are obtained from the *open-shell* orbitals of excited states, which are solutions of the Hartree-Fock-Roothaan Hamiltonians. In these orbitals we find considerable σ bonding and a smaller π bonding, significant fluoride s - p hybridization, and a small expansion of the $3d$ orbitals which is greater in the t_{2g} than in the e_g orbitals. Allowing for spin-polarization correlation in the unrestricted calculations, however, adds important contributions to transferred hyperfine interactions and neutron form factors.

I. INTRODUCTION

Continued interest in the optical, magnetic, and structural properties of transition-metal compounds arising from the occurrence of unfilled shells as-

sociated with the metal-ion $3d$ electrons has led to a wide variety of attempts at theoretical explanation. Recent theoretical emphasis has concentrated on clusters containing the transition-metal ion surrounded by its nearest-neighbor anions or ligands

as being representative of the crystal. Early theoretical efforts which concentrated only on the transition-metal ion, while explaining individual physical properties, were inadequate for any consistent understanding of the entire range of behavior. For this reason, early attempts to compute *ab initio* the crystal-field-splitting parameter $10Dq$ failed. Also, the interpretation of properties such as partial quenching of orbital angular momentum, magnetic hyperfine interactions, and neutron magnetic scattering experiments established unambiguously the important role played by the neighboring anions or ligands. More recently, the role of cluster models has been emphasized in connection with explaining the magnetic interaction between metal ions.¹

The molecular-orbital (MO) formulation originally proposed by Van Vleck² naturally allows for covalent bonding and a redistribution of electronic charge, evidently necessary to explain the experimental data. Subsequent development of semiempirical MO schemes resulted from the obvious numerical difficulties inherent in any completely *ab initio* calculation.³ In the first detailed nonempirical calculation, Sugano and Shulman⁴ obtained a reasonable value for $10Dq$ and other experimental parameters by assigning the $3d$ electrons in NiF_6^{-4} to antibonding linear combination of atomic orbitals (LCAO) MO's. The coefficient of the F^- ligand orbitals or "covalency parameters" were determined from the solutions of the ionic Hartree-Fock one-electron Hamiltonian. However, it is well known⁵⁻⁹ that it is the one-electron Hamiltonian of the bonding orbitals whose spin is antiparallel to the occupied antibonding orbitals which determines the extent of covalency in a minimal basis. When the one-electron Hamiltonian of Sugano and Shulman was corrected by subsequent workers,⁵ they failed to obtain agreement with experiment.

Several important questions can be raised. First what are the results of solving the many-electron open-shell self-consistent-field (SCF) equations for the ground and various excited states and how do they compare to closed-shell or pseudo-closed-shell calculations? Second, what are the effects of obtaining self-consistency starting with an ionic Hartree-Fock Hamiltonian, of electronic reorganization, and of limited configuration interaction? Third what are the effects of using a basis other than the free-ion basis used by Sugano and Shulman?¹⁰⁻¹³ Is there a notable polarization of free-ion metal or ligand orbitals in a slightly extended basis? And finally, what are the significant effects of relaxing spin restrictions?

Some of these questions were approached by Ellis, Freeman, and Ros,⁹ who solved the unrestricted Hartree-Fock equations using a one-center basis of Slater-type orbitals. However, although the one-center basis provides a great simplifica-

tion in the calculation of integrals, it was thought to be a serious compromise to the more accurate multicenter atomic orbital basis. Alternatively, we choose to use a multicenter basis and approximate the resulting three- and four-center integrals which, if computed, would consume considerable computer time. In this way we make a basic departure from those previous calculations which have made approximations in the one-electron Hamiltonians rather than in the integrals.

In this paper we present the results of open-shell LCAO-MO-SCF calculations on various many-electron states of the NiF_6^{-4} cluster. We use a slightly extended multicenter atomic orbital basis and block diagonalize the Fock operators in the usual way by the use of symmetry orbitals. A limited $d-d$ configuration interaction is employed. Recently, Richardson, Vaught, Soules, and Powell¹⁴ presented preliminary calculations on the octahedral clusters TiF_6^{-3} , CrF_6^{-3} , FeF_6^{-4} , and NiF_6^{-4} . Because these authors consistently obtained excellent agreement with the experimental fluoride absorption spectra, we wish to examine in some detail the method and approximations. In particular, the approach based on the many-electron Hartree-Fock-Roothaan equations is contrasted with the more familiar orbital picture. We show the effect of electron delocalization on the electrostatic interactions among the essentially $3d$ molecular orbitals and discuss in some detail the contributions to optical transition energies.

In Sec. II, we sketch the application of the open-shell SCF procedure to states of the d^8 configuration in octahedral NiF_6^{-4} clusters and define the basis sets used in these calculations. In Sec. III, wave functions and the $d-d$ spectrum of NiF_6^{-4} are presented as calculated using various bases and modifications of the integral approximations. Contributions to $10Dq$ and the causes and effects of electron delocalization are analyzed in Sec. IV. In Sec. V, we present the results of an unrestricted Hartree-Fock calculation and compare the magnetic hyperfine interactions and neutron form factors in Sec. VI.

II. APPLICATION OF OPEN-SHELL SCF METHOD

A detailed discussion of the basic open-shell SCF theory as applied to octahedral transition-metal clusters is given elsewhere.¹⁵ A summary is presented here, however, in order better to discuss the results of these calculations. The use of a cluster in an external crystalline potential as a model for octahedral transition-metal fluorides assumes that the electrons of interest are localizable in the pseudomolecule and specifically neglects the periodicity of the lattice. Nevertheless, this model is suggested by many experimental and theoretical considerations. For instance, it is well known that

the purely electronic optical transition energies are affected very little by structural changes beyond the nearest-neighbor anions. In the systems KNiF_3 ,¹⁶ KZnF_3 :Ni,¹⁷ KMgF_3 :Ni,¹⁸ and NiF_2 ,¹⁹ the positions of the transitions vary by less than a few hundred cm^{-1} . On theoretical grounds, the cluster model represents a partitioning in the ground-state or closed-shell Hartree-Fock Hamiltonian of the crystal which is accurate to terms of the order δ^2 , where δ is the mixing parameter between basis functions on neighboring ions.⁹ Hence it is a good approximation in highly ionic crystals and with the use of a localized basis. For excited states, the cluster model represents a localized molecular excitation.

A. Wave Function and Total Energy

In the MO approach the wave function is written as a linear combination of Slater determinants of one-electron MO functions.²⁰ In the LCAO approximation, the MO's, ϕ 's, are expanded in an orthogonalized atomic orbital basis (χ) which is transformed to a set of functions, λ 's, belonging to particular rows (γ) of irreducible representations (Γ) of the appropriate point group:

$$\phi_{i\Gamma\gamma} = \sum_k \lambda_{k\Gamma\gamma} C_{ki\Gamma} \quad (2.1)$$

Wave functions for states belonging to different symmetry species are automatically orthogonal. Those belonging to the same species are orthogonal if constructed from the same set of orthogonal MO's.

The principal configurations of interest are

$$(A) (1a_{1g})^2 (1e_g)^4 (1t_{1u})^6 (2a_{1g})^2 (2t_{1u})^6 (2e_g)^4 (3t_{1u})^6 \\ \times (1t_{2g})^6 (1t_{1g})^6 (1t_{2u})^6 (2t_{2g})^x (3e_g)^y \quad (2.2)$$

where a_{1g} , e_g , t_{1u} , t_{2g} , t_{1g} , and t_{2u} label irreducible representations of O_h in the Mulliken-Placek notation, and $x + y = 8$.

(A) contains the localized inner-shell²¹ or "core" orbitals. It is possible within the framework of present programs to include the 3s and 3p orbitals in the valence set. This would have the effect of explicitly orthogonalizing them to the ligand orbitals.

These core orbitals are assumed to contribute little to optical transition energies which arise from transitions in the largely 3d antibonding orbitals ($2t_{2g}$) and ($3e_g$). We therefore describe them as free-ion orbitals in the "frozen" core approximation, so that

$$(A) = (1s_{N1})^2 (2s_{N1})^2 (2p_{N1})^2 (1s_{F1})^2 (1s_{F2})^2 (1s_{F3})^2 \\ \times (1s_{F4})^2 (1s_{F5})^2 (1s_{F6})^2 (3s_{N1})^2 (3p_{N1})^6$$

The total valence-shell electronic energy in the spin-restricted Born-Oppenheimer nonrelativistic approximation is given by^{15,21}

$$E(t^x e^y; S\Gamma) = \underline{H}^0 \underline{D}_t^\dagger + \frac{1}{2} \underline{D}_t (\mathcal{J} - \frac{1}{2} \mathcal{K}) \underline{D}_t^\dagger \\ - \frac{1}{2} \underline{D}_o (\mathcal{J} - \frac{1}{2} \mathcal{K}) \underline{D}_o^\dagger + G(x, y; S\Gamma') \quad (2.3)$$

\underline{D}_t and \underline{D}_o are the familiar total (t) and open-shell (o) valence-shell density coefficient matrices (row vectors)

$$\underline{D}_t = \|\underline{D}_t(a_{1g}), \underline{D}_t(t_{1u}), \dots, \underline{D}_t(\Gamma), \dots\|, \\ \underline{D}_o = \|\underline{D}_o(a_{1g}), \underline{D}_o(t_{1u}), \dots, \underline{D}_o(\Gamma), \dots\|, \quad (2.4)$$

with elements

$$\|D_\nu(\Gamma)\|_{ki} = \sum_l C_{ki\Gamma}^* C_{li\Gamma} (2 - \delta_{ki}) n(i\Gamma),$$

where the sum extends over all, or over open shells only, for $\nu = t$ or o , respectively, and $n(i\Gamma)$ is the occupation number of the $i\Gamma$ valence shell. In the core approximation used,

$$\underline{H}^0 = \underline{H} + \underline{V}_{\text{ext}} + \frac{1}{2} \underline{D}_I (\mathcal{J} - \frac{1}{2} \mathcal{K}) \underline{D}_I^\dagger \quad (2.5)$$

\underline{H} is the kinetic plus nuclear attraction energy matrix. $\underline{V}_{\text{ext}}$ is discussed in Sec. II B and \underline{D}_I is the density matrix for the inner shells of the core. The elements in the matrix \underline{H} , and in the supermatrices \mathcal{J} and \mathcal{K} , are defined as usual.^{15,21}

$G(x, y; S\Gamma)$ includes all two-electron electrostatic matrix elements between electrons in the $2t_{2g}$ and $3e_g$ shells. Nine independent integrals may occur in $G(x, y; S\Gamma)$ and a tenth occurs in configuration interaction calculations.²⁰ These integrals reduce to the Slater-Condon integrals F_0 , F_2 , and F_4 or the equivalent Racah parameters A , B , and C only if the $2t_{2g}$ and $3e_g$ MO's were to have purely 3d AO character. In the more general case when those MO's do not have the same radial character, the usual analysis of the energy levels in terms of Racah parameters cannot be made.²² In Table I, we define the set of electrostatic interaction integrals for the $2t_{2g}$ and $3e_g$ MO's which is used in subsequent calculations. In Table II, the coefficients of these integrals appearing in the expression for $G(x, y; S\Gamma)$ are given for all the terms of d^8 .

B. External Potential

The one-electron potential $\underline{V}_{\text{ext}}(\vec{r})$ resulting from the ions external to the cluster was studied extensively by Ellis, Freeman, and Ros.⁹ They include the Madelung potential appropriate to the KNiF_3 structure and corrections for the finite-charge distribution of the surrounding ions. Their conclusion that the external crystal field has very little effect on the cluster wave function was borne out in more approximate preliminary calculations we made that included the external Madelung potential. The localized basis assumed in the cluster model and the near constancy in the region of the cluster of the Coulombic potential which is generated by the rest of an ionic KNiF_3 crystal combine to produce this

TABLE I. Definition of the ten independent $e_e - t_{2g}$ electrostatic interaction integrals, a, b, c

Integral	General MO's	Equivalent AO's
$\bar{J}(tt)$	$\frac{1}{3}(\langle \xi\xi \xi\xi \rangle + \langle \xi\xi \eta\eta \rangle + \langle \xi\xi \zeta\zeta \rangle)$	$A + \frac{5}{3}C$
$\bar{J}(et)$	$\frac{1}{2}(\langle \theta\theta \xi\xi \rangle + \langle \epsilon\epsilon \xi\xi \rangle)$	$A + C$
$\bar{J}(et)$	$\langle \theta\theta \xi\xi \rangle$	$A - 4B + C$
$\bar{J}(ee)$	$\frac{1}{2}(\langle \theta\theta \theta\theta \rangle + \langle \theta\theta \epsilon\epsilon \rangle)$	$A + 2C$
$\bar{K}(tt)$	$\frac{1}{3}(\langle \xi\xi \xi\xi \rangle + \langle \xi\eta \eta\xi \rangle + \langle \xi\zeta \zeta\xi \rangle)$	$\frac{1}{3}A + \frac{10}{3}B + \frac{5}{3}C$
$K(tt)$	$\langle \xi\eta \eta\xi \rangle$	$3B + C$
$\bar{K}(et)$	$\frac{1}{2}(\langle \theta\xi \xi\theta \rangle + \langle \epsilon\xi \xi\epsilon \rangle)$	$2B + C$
$K(et)$	$\langle \theta\xi \xi\theta \rangle$	$4B + C$
$\bar{K}(ee)$	$\frac{1}{2}(\langle \theta\theta \theta\theta \rangle + \langle \theta\epsilon \epsilon\theta \rangle)$	$\frac{1}{2}A + 4B + 2C$
i	$\langle \theta\xi \eta\xi \rangle$	$\sqrt{3}B$

$$^a \langle ab | cd \rangle = \iint a^*(1) b(1) r_{12}^{-1} c^*(2) d(2) dv_1 dv_2.$$

$^b \xi, \eta, \zeta, \theta, \epsilon$ refer to MO's transforming like the d orbitals $d_{yz}, d_{xz}, d_{xy}, d_{x^2-y^2}$, and $d_{x^2+y^2}$, respectively.

$^c A, B$, and C are the Racah parameters, appropriate for the case that all d functions have the same radial function.

result. V_{ext} is therefore neglected in the results presented here.

C. Restricted Open-Shell SCF

In the restricted open-shell SCF procedure, the total energy given in Eq. (2.2) is minimized with respect to variation of the MO coefficients $C_{ki\Gamma}$ subject to the constraint that they remain orthonormal and span irreducible representations of the space and spin symmetry groups. For a given state $t^x e^y s^z \Gamma'$, this leads to the familiar Hartree-Fock-Roothaan equations for closed (c) and open (o) orbitals of the form

$$\begin{aligned} \underline{F}_c \underline{C}(c) &= \sum_j \epsilon(c, j) \underline{SC}(j), \\ \underline{F}_o \underline{C}(o) &= \sum_j \epsilon(o, j) \underline{SC}(j), \end{aligned} \quad (2.6)$$

where

$$\underline{F}_c = \underline{H}^0 + \underline{D}_t \left(\mathcal{J} - \frac{1}{2} \mathcal{K} \right),$$

$$\underline{F}_o = \underline{F}_c - \underline{Q}_o,$$

and \underline{Q}_o is such that

$$\frac{1}{2} \underline{D}_o \underline{Q}_o = \frac{1}{2} \underline{D}_o \left(\mathcal{J} - \frac{1}{2} \mathcal{K} \right) \underline{D}_o^\dagger - G(x, y; \text{ST}').$$

$C(i)$ is the coefficient vector for the i th occupied MO, here spanning the entire basis. These matrices, as written here, actually have block (diagonal) form according to the various MO symmetry species.

In the Roothaan formulation, off-diagonal Lagrangian multipliers connecting closed-shell orbitals having the same Fock operator are eliminated by a unitary transformation. Those connecting closed- and open-shell orbitals both belonging to some representation Γ are removed by means of the coupling operators^{23,24}

$$\underline{R}_c(\Gamma) = n_o(\Gamma) [n_o(\Gamma) - n_c(\Gamma)]^{-1} \sum_{\text{open}} [\underline{T}_i(\Gamma) + \underline{T}_i^\dagger(\Gamma)], \quad (2.7)$$

$$\underline{R}_o(\Gamma) = n_o(\Gamma) [n_o(\Gamma) - n_c(\Gamma)]^{-1} \sum_{\text{closed}} [\underline{T}_i(\Gamma) + \underline{T}_i^\dagger(\Gamma)].$$

$\underline{T}_i(\Gamma)$ is that segment of the matrix $\underline{SC}(i) \underline{C}^\dagger(i) \underline{Q}_o^\dagger$ associated with MO's belonging to Γ . By this means and by taking explicit note of block diagonal forms, Eqs. (2.6) may be written

$$\begin{aligned} (\underline{F}_c + \underline{R}_o) \underline{C}_c &= \underline{\epsilon}_c \underline{SC}_c, \\ (\underline{F}_o + \underline{R}_c) \underline{C}_o &= \underline{\epsilon}_o \underline{SC}_o, \end{aligned} \quad (2.8)$$

with one pair of equations for each MO symmetry species. Here $\underline{\epsilon}_c, \underline{\epsilon}_o$ are diagonal eigenvalue matrices, and \underline{C}_c and \underline{C}_o are the eigenvectors of the closed and open MO's, respectively, belonging to Γ . If no open shells occur in a symmetry species, \underline{R}_o vanishes and the second equation is ignored.

TABLE II. Coefficients in the $e_g - t_{2g}$ electrostatic interaction energy matrix.^a $G(x, y; \text{ST}') = \alpha_1 \bar{J}(tt) + \beta_1 \bar{K}(tt) + \gamma_1 K(tt) + \alpha_2 \bar{J}(et) + \beta_2 \bar{K}(et) + \gamma_2 J(et) + \delta_2 K(et) + \alpha_3 \bar{J}(ee) + \beta_3 \bar{K}(ee)$.

State	Config	α_1	β_1	γ_1	α_2	β_2	γ_2	δ_2	α_3	β_3	Off-diagonal element
$^3A_{2g}$	$t^6 e^2$	18	-9	0	12	-6	0	0	2	-2	...
$^3T_{2g}$	$t^5 e^3$	12	-6	0	14	-7	1	-1	4	-2	...
$^3T_{1g}$	$t^5 e^3$	12	-6	0	16	-9	-1	+1	4	-2	$2(\sqrt{3})i$
	$t^4 e^4$	$\frac{15}{2}$	$-\frac{3}{2}$	0	16	-8	0	0	8	-4	
$^1T_{2g}$	$t^5 e^3$	12	-6	0	14	-7	1	1	4	-2	$2i$
	$t^4 e^4$	$\frac{15}{2}$	$-\frac{3}{2}$	2	16	-8	0	0	8	-4	
$^1T_{1g}$	$t^5 e^3$	12	-6	0	16	-5	-1	-1	4	-2	...
1E_g	$t^6 e^2$	18	-9	0	12	-6	0	0	1	0	$\sqrt{3} [\bar{K}(et) - K(et)]$
	$t^4 e^4$	6	0	-3	16	-8	0	0	8	-4	
$^1A_{1g}$	$t^6 e^2$	18	-9	0	12	-6	0	0	0	2	$\sqrt{6} \bar{K}(et)$
	$t^4 e^4$	6	0	0	18	-8	0	0	8	-4	

^aSee Table I for definitions of the integrals.

The original formulation of Roothaan²¹ applied to only a limited number of systems containing only one open shell. However, it is fairly easy to generalize this method to cover all the states of interest in the octahedral transition complexes.¹⁵

D. Unrestricted Open-Shell SCF

The spin-polarized (SP) procedure, a type of unrestricted SCF procedure in which electrons of opposite spin are allowed to occupy different orbitals, has also been discussed extensively.²⁵ For systems containing only filled and half-filled shells, the unrestricted Hartree-Fock-Roothaan equations analogous to (2.6) are given by

$$\begin{aligned}\underline{F}, \underline{C}, (i) &= \underline{\epsilon}, \underline{S}, \underline{C}, (i), \\ \underline{F}, \underline{C}, (i) &= \underline{\epsilon}, \underline{S}, \underline{C}, (i),\end{aligned}\quad (2.9)$$

where the arrows label electron spin and where

$$\underline{F}_s = \underline{H}^0 + \underline{D}_s \mathcal{J} - \underline{D}_s \mathcal{K},$$

$$\underline{F}_i = \underline{H}^0 + \underline{D}_i \mathcal{J} - \underline{D}_i \mathcal{K}.$$

The spin density matrices \underline{D}_s and \underline{D}_i are defined as in Eqs. (2.4) but with elements

$$\|D_s(\Gamma)\|_{kl} = \sum_{i \text{ occupied}} C_{ki\Gamma s}^* C_{li\Gamma s} (2 - \delta_{kl}) n_s(i\Gamma),$$

with $s = \uparrow$ or \downarrow , respectively.

Off-diagonal multipliers between orbitals of opposite spin vanish directly so that only unitary transformations are required to eliminate all off-diagonal multipliers. However, this transformation is different from that used in the Roothaan spin-restricted formulation discussed above, so that the one-electron MO's and energies appear different even when a minimal basis is used, although both wave functions give the same values for physical observables.

E. Bases and Integral Approximations

Of the various possible analytical bases used in molecular Hartree-Fock calculations, multicenter Slater-type bases have proved to be accurate and reliable.¹⁴ In Table III, we give the STO exponents used in these calculations. The D basis for the cluster includes a double- ζ function to represent the critical 3d orbitals.²⁶ Calculations designated DSP include the metal-ion 4s and 4p orbitals, which, because of their large radial extent, supplement the ligand orbitals in the region between the metal and ligand ions. Calculations labeled DDSP together include the 3d_i functions, which are the 3d STO's with the larger orbital exponent [$\zeta(3d_i) = 5.75$] and which permit a limited radial 3d distortion. The double- ζ 3d function closely approximates the more accurate Hartree-Fock free-ion function computed by Watson.²⁶

Independent elements of the overlap matrices $S(\Gamma)$ are included in Table IV.

The selection of a basis for the cluster is arbitrary. It is well known that a small multicenter Slater-type basis in which all the parameters are varied provides a good approximation to the Hartree-Fock solution. However, it is not yet practical to vary the exponential factors because of the large amount of computer time required. How good the present choice is can only be indicated by the accuracy of the results of the calculations.

Of the required integrals over the basis which appear in the Fock matrices of Eqs. (2.8) and (2.9), all one- and two-center integrals were obtained exactly. Because of the large amount of computer time required to evaluate all three- and four-center integrals, these were uniformly approximated. All integrals containing products of two AO's on different fluoride ions are small and were uniformly neglected. This approximation assumes that there is negligible interpenetration of adjacent fluoride AO's and has been used by previous authors.^{4,5-8} Second, all remaining three-center integrals were approximated using the Mulliken approximation.²⁷ In the REG calculations, using the regular Mulliken approximation, the charge distribution on two of the three centers is expanded according to

$$\chi_a \chi_b \approx \frac{1}{2} \langle \chi_a | \chi_b \rangle (\chi_a^2 + \chi_b^2), \quad (2.10)$$

thus reducing the calculation of three-center integrals to the evaluation of overlap integrals $\langle \chi_a | \chi_b \rangle$ and a sum of two-center integrals. The MOD calculations are the same, except that each overlap integral was replaced in this approximation by a factor determined from relationships among exactly computed two-center two-electron integrals. In the 3CEN calculations, the overlap integral was replaced by a factor which made the one-electron three-center

TABLE III. Orbital exponents of the Ni²⁺ and F⁻ STO basis.^{a,b}

Center	$\chi(nl)$	$\zeta(nl)$
Ni ²⁺	1s	27.37
	2s	10.60
	3s	4.90
	4s	1.70
	2p	11.50
	3p	4.60
	4p	1.34
	3d _i	5.75
	3d _o	2.40
F ⁻	1s	8.7
	2s	2.425
	2p	2.425

^aThe "double- ζ " 3d basis function is $0.59589 \chi(3d_i) + 0.54969 \chi(3d_o)$.

^bThe Ni-F distance used is 3.79 a.u. = 2.006 Å.

TABLE IV. Overlap matrix elements.^a

Metal	Ligand symmetry-adapted orbital		
	2s	2p σ	2p π
4p	0.519 07	0.200 65	0.188 78
4s	0.476 08	0.314 75	...
3d	0.087 80	0.103 33	0.043 00
3d _t	0.008 43	0.005 09	0.002 19
3s	0.019 43	0.031 40	...
3p	0.015 03	0.024 00	0.004 57

^aS(3d, 3d_t) = 0.883 49.

ter integrals exact; the same factors were then used in the two-electron integrals. The nature and accuracy of the integral and the frozen core approximations have been investigated in greater detail over a range of internuclear distances in connection with similar calculations on other clusters.^{14,15} Detailed results and interpretations will be presented subsequently. In brief, however, we note the following conclusions. Essentially the same results for fluoride clusters are produced by using the three integral approximations and also, in the case of TiF₆⁻³, by using more accurate three-center integrals. Likewise, we find that the neglect of two-center overlap distributions between ligand AO's has little consequence for fluoride clusters at their equilibrium geometry. Since valence AO's used in all three bases are taken orthogonal to all orbitals on the same center, no problems occur in that respect.

With no further approximations, we solve the SCF pseudoeigenvalue equations (2.8) and (2.9) for the ground and various excited states iteratively to a convergence of 10⁻⁴ in the vector coefficients. Convergence was usually easily reached beginning with a set of ionic trial vectors.

III. OPTICAL TRANSITION ENERGIES AND WAVE FUNCTIONS

The electronic absorption spectrum of KNiF₃ has been analyzed.¹⁶ Its rich detail provides considerable information which must be explained by any theory proposing to describe the effects of covalency in these compounds. Five absorption bands are observed and have been assigned to transitions from the ground electronic state ³A_{2g} to ³T_{2g}, ^a³T_{1g}, ¹E_g, and ^b³T_{1g} in order of increasing energy. The ³A_{2g} - ³T_{2g} transition is magnetic dipole allowed.

The no-phonon line accompanied by a diffuse phonon sideband is observed at low temperatures. The spin-orbit split transitions have been resolved¹⁸ and the spin-orbit coupling parameter has a value in the range of 305-320 cm⁻¹. The other four bands are forced-electric dipole in character, and the spin-allowed ³T_{1g} bands reveal sharp vibronic progressions at low temperatures which have been assigned to lattice vibrations.¹⁸

Since the ground- and excited-state energies were computed at the same internuclear distance, the calculated transition energies should be compared to the vertical transition, corresponding to the maximum in the absorption band at low temperatures. Also, it has been pointed out that this corresponds only to a rough average over the spin-orbit components. A more accurate value of the vertical 10Dq, in which there was compensation for spin-orbit splitting, is around 7400 cm⁻¹.¹⁸

A. Computed Transition Energies

In Table V, we show a comparison of our calculated results and the experimental energy levels. They are seen to be accurate to within 10-20% for the five observed transitions. The largest deviations occur for the higher-energy transitions which are computed to be too large.

The energies of the (³T_{2g}, ³T_{1g}) and (¹T_{2g}, ¹T_{1g}) pairs were obtained from the SCF solutions for the average states $T_{av} = \frac{1}{2}(T_{2g} + T_{1g})$ which were then separated by adding the appropriate electrostatic integrals. The latter unaveraged Coulomb and exchange integrals $J(et)$ and $K(et)$ were assumed to be reduced from their free-ion values by the same ratio as their averaged counterparts, $\bar{J}(et)$ and $\bar{K}(et)$. Since these are very close to their free-ion values, this is probably a good approximation. Energies for the other singlet states were computed from the $t^5e^3{}^1T_{av}$ SCF results. All excited-state energies are given relative to the independent SCF total energy of the ³A_{2g} ground state.

The calculated ³T_{1g}, ¹E_g, ¹T_{2g}, ¹A_{1g} term energies contain the usual *d-d* configuration interaction.²⁸ The strong field energy expressions neglecting spin-orbit interactions have been given by Tanabe and Sugano in terms of the Racah parameters.²² In terms of our more general O_h electrostatic matrix elements, they are the eigenvalues of the matrix

$$\begin{vmatrix} E(t^5e^3; S\Gamma) - E(t^6e^2; {}^3A_{2g}) & E'(S\Gamma) \\ E'(S\Gamma) & E(t^4e^4; S\Gamma) - E(t^6e^2; {}^3A_{2g}) \end{vmatrix}, \quad (3.1)$$

where $E(t^*e^j; S\Gamma)$ are the single-configuration energies and $E'(S\Gamma)$ is the off-diagonal matrix element given in Table II. In Table V, calculations

with and without configuration interaction are compared. Also, the coefficients of the configurations appearing in the wave function are given.

TABLE V. Best calculated spectral transition energies (in cm^{-1}) for NiF_6^{-4} (REG).

Transition	Without CI		With CI				Expt ^b
	Energies		Coefficients ^a		Energies		
	D	DSP	D	DSP	D	DSP	
t^6e^2 $^3A_{2g}$					
t^5e^3 $^3T_{2g}$	7 977	7 210			7 977	7 210	7 250
a^3T_{1g}	23 340	22 980	$\left\{ \begin{array}{l} 0.6278 \\ -0.7784 \end{array} \right\}$	$\left\{ \begin{array}{l} 0.6020 \\ -0.7985 \end{array} \right\}$	13 740	12 480	12 530
a^1E_g	19 360	20 050	$\left\{ \begin{array}{l} 0.9754 \\ 0.2206 \end{array} \right\}$	$\left\{ \begin{array}{l} 0.9677 \\ 0.2520 \end{array} \right\}$	18 380	18 870	15 440
a^1T_{2g}	27 450	27 390	$\left\{ \begin{array}{l} 0.9355 \\ -0.3534 \end{array} \right\}$	$\left\{ \begin{array}{l} 0.9208 \\ -0.3899 \end{array} \right\}$	25 790	25 460	20 920
b^3T_{1g}	19 990	18 450	$\left\{ \begin{array}{l} 0.7784 \\ 0.6278 \end{array} \right\}$	$\left\{ \begin{array}{l} 0.7985 \\ 0.6020 \end{array} \right\}$	29 590	28 950	23 810
a^1A_{1g}	37 990	39 870	$\left\{ \begin{array}{l} 0.8925 \\ -0.4510 \end{array} \right\}$	$\left\{ \begin{array}{l} 0.8755 \\ -0.4832 \end{array} \right\}$	29 200	29 820	
t^5e^3 $^1T_{1g}$	32 600	32 640	32 600	32 640	
b^1E_g	37 470	36 200	$\left\{ \begin{array}{l} 0.2206 \\ -0.9754 \end{array} \right\}$	$\left\{ \begin{array}{l} 0.2520 \\ -0.9677 \end{array} \right\}$	38 440	37 380	
b^1T_{2g}	37 470	36 200	$\left\{ \begin{array}{l} 0.3534 \\ 0.9355 \end{array} \right\}$	$\left\{ \begin{array}{l} 0.3899 \\ 0.9208 \end{array} \right\}$	39 130	38 130	
b^1A_{1g}	63 650	62 810	$\left\{ \begin{array}{l} 0.4510 \\ 0.8925 \end{array} \right\}$	$\left\{ \begin{array}{l} 0.4832 \\ 0.8755 \end{array} \right\}$	72 440	72 860	

^aThe upper number in each pair of entries is the coefficient of the t^5e^3 configuration, and the lower, of the t^4e^4 configuration.

^bReference 16.

The most prominent effect of configuration interaction is in lowering a^3T_{1g} below a^1E_g , in agreement with experiment. The a^3T_{1g} state is largely t^4e^4 in character. This would explain why it has a broader band than the b^3T_{1g} band which, although it is higher in energy, is mainly t^5e^3 . Extending the configuration interaction calculation by including charge-

transfer configurations undoubtedly would improve agreement with experiment, particularly for the higher-lying states.

In Table VI, we compare the computed spectra using various approximations discussed earlier, looking first at the spectra computed from the ${}^3T_{av}$ SCF results. The first row, which gives the posi-

TABLE VI. Calculated $d-d$ transition energies (in eV) as a function of basis, integral approximation, and reference SCF state.^a

	From ${}^3A_{2g}$ REG D	From ${}^1T_{av}$ REG D	From ${}^3T_{av}$						
State	D	D	REG D	REG DSP	REG DDSP	MOD D	MOD DSP	3CEN D	3CEN DSP
$t^6e^2\ {}^3A_{2g}$	0.000	0.090	0.010	0.003	0.019	0.010	0.003	0.011	0.003
$t^5e^3\ {}^3T_{2g}$	1.787	1.024	0.989	0.894	1.022	1.000	0.873	1.054	0.916
a^3T_{1g}	2.909	1.719	1.703	1.547	1.749	1.720	1.512	1.808	1.583
a^1E_g	2.334	2.279	2.263	2.339	2.329	2.264	2.328	2.261	2.335
a^1T_{2g}	4.058	3.197	3.206	3.159	3.248	3.216	3.128	3.272	3.179
b^3T_{1g}	4.833	3.659	3.668	3.589	3.702	3.680	3.553	3.754	3.613
a^1A_{1g}	3.938	3.621	3.634	3.707	3.716	3.638	3.686	3.650	3.708
$t^5e^3\ {}^1T_{1g}$	4.842	4.041	4.061	4.054	4.107	4.069	4.023	4.117	4.068
b^1E_g	6.253	4.766	4.779	4.638	4.785	4.793	4.591	4.900	4.674
b^1T_{2g}	6.319	4.852	4.867	4.732	4.871	4.880	4.684	4.985	4.767
b^1A_{1g}	10.235	8.980	9.052	9.060	9.044	9.056	9.005	9.139	9.076

^aNote that the energies calculated for the ${}^3A_{2g}$ state represent energies *above* the SCF energy of that state. These quantities reflect the (slight) differences among the SCF MO's for the ground and excited states.

TABLE VII. Restricted HF MO coefficients and orbital energies for the ${}^3A_{2g}$ and ${}^3T_{av}$ states of MiF_6^{-4} (REG).

State	MO	ϵ (a.u.)	$nl(Ni)$	Symmetry-orbital coefficients			
				$3d_i(Ni)$	$2s(F)$	$2p\sigma(F)$	$2p\pi(F)$
${}^3A_{2g}$	(a) D Basis				0.9999	0.0147	
	$1a_{1g}$	-0.42217			-0.0147	0.9999	
	$2a_{1g}$	0.53212			0.9999	0.0143	0.0000
	$1t_{1u}$	-0.42202			-0.0143	0.9999	0.0053
	$2t_{1u}$	0.53324			0.0000	-0.0053	1.0000
	$3t_{1u}$	0.55182			0.9970	0.0174	
	$1e_g$	-0.42370	0.0279		-0.0420	0.9617	
	$2e_g$	0.49473	0.1917		-0.1130	-0.2928	
	$3e_g$	0.26335	0.9906				
	$1t_{2g}$	0.55964	-0.1642				0.9953
	$2t_{2g}$	0.26599	0.9874				0.1216
	$1t_{1g}$	0.55184					1.0000
$1t_{2u}$	0.55183					1.0000	
${}^3T_{av}$	$1a_{1g}$	-0.42071			0.9999	0.0154	
	$2a_{1g}$	0.55222			-0.0154	0.9999	
	$1t_{1u}$	-0.42067			0.9999	0.0152	-0.0000
	$2t_{1u}$	0.53285			-0.0152	0.9999	0.0014
	$3t_{1u}$	0.55397			0.0001	-0.0014	1.0000
	$1e_g$	-0.42248	0.0299		0.9967	0.0193	
	$2e_g$	0.48374	0.2101		-0.0465	0.9560	
	$3e_g$	0.32075	0.9868		-0.1110	-0.3106	
	$1t_{2g}$	0.54261	0.0997				0.9907
	$2t_{2g}$	0.26722	0.9960				-0.1423
	$1t_{1g}$	0.55391					1.0000
	$1t_{1u}$	0.55397					1.0000
${}^3A_{2g}$	(b) DSP Basis				0.9748	-0.0208	
	$1a_{1g}$	-0.50756	0.0511		-0.2357	0.7745	
	$2a_{1g}$	0.35913	0.4701		0.9851	-0.0108	-0.0017
	$1t_{1u}$	-0.50893	0.0282		-0.2149	0.5495	0.6298
	$2t_{1u}$	0.39434	0.4011		-0.0242	0.7232	-0.6877
	$3t_{1u}$	0.46995	0.0568		0.9980	-0.0150	
	$1e_g$	-0.50853	0.0197		-0.0020	0.9763	
	$2e_g$	0.45883	0.1379		-0.1090	-0.2396	
	$3e_g$	0.39274	0.9997				
	$1t_{2g}$	0.39326	0.8390				0.5093
	$2t_{2g}$	0.49874	-0.5458				0.8617
	$1t_{1g}$	0.46088					1.0000
$1t_{2u}$	0.46167					1.0000	
${}^3T_{av}$	$1a_{1g}$	-0.50648	0.0520		0.9743	-0.0206	
	$2a_{1g}$	0.35919	0.4710		-0.2369	0.7738	
	$1t_{1u}$	-0.50790	0.0287		0.9848	-0.0105	-0.0017
	$2t_{1u}$	0.39499	0.4026		-0.2161	0.5532	0.6253
	$3t_{1u}$	0.47064	0.0522		-0.0221	0.7208	-0.6906
	$1e_u$	-0.50754	0.0206		0.9979	-0.0141	
	$2e_g$	0.45395	0.1459		-0.0039	0.9744	
	$3e_g$	0.45415	0.9985		-0.1096	-0.2473	
	$1t_{2g}$	0.46311	0.0641				0.9952
	$2t_{2g}$	0.41784	0.9989				-0.1069
	$1t_{1g}$	0.46241					1.0000
	$1t_{2u}$	0.46324					1.0000

tion of the ground state computed from the particular SCF results, indicates the small amount of reorganization energy in these cases. The three-center Mulliken integral approximations are compared and no significant difference is found for the DSP basis. For the smallest basis D the transition energies are raised in going from the REG to the MOD to the 3CEN approximation. Also the relative loca-

tion of the a^1A_{1g} state is shifted. We have no explanation for these effects. The more flexible DSP basis gives consistently better agreement with experiment, but the further inclusion of the $3d_i$ functions raises the energy of the ${}^3T_{2g}$ and a^3T_{1g} states, by approximately 0.1 and 0.2 eV, respectively.

Table VI also exhibits spectra computed from the $t^5e^3{}^3T_{av}$ state and the ${}^3A_{2g}$ ground-state SCF results.

TABLE VII (continued).

State	MO	ϵ (a.u.)	$nI(\text{Ni})$	Symmetry-orbital coefficients			
				$3d_i(\text{Ni})$	$2s(\text{F})$	$2p\sigma(\text{F})$	$2p\pi(\text{F})$
$^3A_{2g}$	$1a_{1g}$	-0.50909	0.0500	(c) DDSP Basis	0.9753	-0.0229	
	$2a_{1g}$	0.35953	0.4695		-0.2328	0.7749	
	$1t_{1u}$	-0.51036	0.0278		0.9853	-0.0133	-0.0016
	$2t_{1u}$	0.39341	0.3993		-0.2123	0.5389	0.6404
	$3t_{1u}$	0.46962	0.0659		-0.0273	0.7300	-0.6793
	$1e_g$	-0.51040	0.0314	-0.0106	0.9970	-0.0172	
	$2e_g$	0.44855	0.2469	-0.0905	-0.0111	0.9608	
	$3e_g$	0.35373	0.9783	0.0191	-0.1097	-0.2647	
	$1t_{2g}$	0.48824	-0.4300	-0.0169			0.9142
	$2t_{2g}$	0.36420	0.9499	-0.0606			0.4035
	$1t_{1g}$	0.45862					1.0000
	$1t_{2u}$	0.45948					1.0000
$^3T_{av}$	$1a_{1g}$	-0.50782	0.0511		0.9747	-0.0225	
	$2a_{1g}$	0.35919	0.4708		-0.2345	0.7740	
	$1t_{1u}$	-0.50916	0.0284		0.9850	-0.0127	-0.0017
	$2t_{1u}$	0.39403	0.4016		-0.2141	0.5456	0.6329
	$3t_{1u}$	0.47024	0.0590		-0.0241	0.7258	-0.6847
	$1e_g$	-0.50921	0.0319	-0.0100	0.9969	-0.0160	
	$2e_g$	0.44258	0.2501	-0.0845	-0.0130	0.9591	
	$3e_g$	0.41838	0.9951	-0.0013	-0.1119	-0.2751	
	$1t_{2g}$	0.38249	0.1227	-0.0482			0.9914
	$2t_{2g}$	0.45790	1.0337	-0.0409			-0.1247
	$1t_{1g}$	0.46056					1.0000
	$1t_{2u}$	0.46147					1.0000

The spectrum computed from the $^1T_{av}$ state is in essential agreement with that computed from the $^3T_{av}$ and from the separate SCF calculations. There is found only a slightly larger electronic reorganization energy. However, the spectrum computed from the ground state is not in agreement with the others. The reason for this can be seen upon comparing the vector coefficients obtained for the $^3A_{2g}$ and the $^3T_{av}$ states as given in Table VII. Although the a_{1g} , t_{1u} , and e_g MO's have essentially the same character whether computed from the ground- or excited-state SCF's, the closed-shell t_{2g} MO's are apparently more mixed or "covalent" in the ground-state t^6 calculation. More will be said about this in Sec. IV. This result forces us to reject any spectral calculation based on a closed-shell or pseudo-closed-shell Hamiltonian, although, of course, the total energy is significant.

B. Wave Functions

Table VII displays the vector coefficients and eigenvalues for the three bases used in our calculations; only those for the REG Mulliken approximation are given, since no significant difference is found in either of the modified Mulliken approximations.

Because of the physical importance of the $3e_g$ and $2t_{2g}$ MO's, we briefly discuss the character of these orbitals. From Table VII the so-called covalency or ligand mixing parameters for the (D, DSP, DDSP)

bases are (-0.113, -0.109, -0.110) and (-0.293, -0.240, and -0.265) for the fluoride $2s$ and $2p\sigma$ symmetry-adapted functions, respectively. These values can be compared with the theoretical values obtained by Offenhartz⁸ using Sugano and Shulman's basis,⁴ -0.105 and -0.222, respectively, and also with experimentally determined parameters by Shulman and Knox,²⁹ namely, -0.116 and -0.337, respectively. These comparisons are only qualitative, since the two theoretical sets are derived from different fluoride bases, and the "experimental" values incorporate a number of assumptions. Nevertheless, it is noted that the $2s$ coefficients are very similar and that our $2p$ coefficients are intermediate between those of Offenhartz and of Shulman and Knox and differ less among themselves than with the other two. In a more reliable test of covalency, we give the results of directly computing the hyperfine interactions from our wave function in Sec. VI.

In contrast to the $3e_g$ orbitals, the $2t_{2g}$ open-shell orbitals participate in a much smaller π bonding. From the $^3T_{av}$ SCF results, the fluoride $2p\pi$ symmetry-adapted orbital coefficients are (-0.142, -0.107, -0.125) for the three bases. We emphasize that this coefficient has physical meaning only when the t_{2g} orbitals are not fully occupied as in the excited state $^3T_{2g}$.

Whereas our results indicate that the $3dt$ orbitals participate in less covalent bonding or electron de-

localization, they are better described as radially slightly expanded. From Table VII, the coefficients of the $3d_i$ STO's are -0.0409 and -0.0013 for the $2t_{2g}$ and $3e_g$ MO's, respectively, of the ${}^3T_{av}$ state. These very small negative coefficients indicate only a slight expansion from the free-ion radial function. This result is important because properties which depend on the shape of the $3d$ orbitals may be relatively insensitive to a small electron delocalization and vice versa. For instance, spin-orbit coupling and neutron magnetic scattering are strongly affected by the shape of the $3d$ orbitals. Recently, Freeman and Ellis³⁰ and Soules and Richardson³¹ in independent unrestricted Hartree-Fock calculations have shown that an expansion of the $3dt$ orbitals in the cluster $MnF_6^{-4} (2t_{2g})^3(3e_g)^2$ can explain the observed contraction of the neutron form factor. This effect is not observed for the Ni salts, which do not have unpaired t_{2g} electrons. Also, the spin-orbit coupling parameter is only slightly reduced from its free-ion value 324 cm^{-1} .

Of interest in discussing the wave function is the Mulliken gross population analysis which divides the electronic charge arbitrarily into atomic basis functions. This is shown in Table VIII. Of particular importance is the charge transferred to the vacant metal-ion $3d$ orbitals. In going from the bases labeled D to DSP to DDSP, this charge at first decreases when electronic reorganization is allowed in the $4s$ and $4p$ orbitals but it increases again when additional variational freedom is given to the $3d$ function by the inclusion of the $3d_i$.

There is a greater differential increase in charge transferred to the $3de$ orbitals than to the $3dt$ orbitals in the $t^5e^3{}^3T_{av}$ state, which has one vacant orbital in each MO symmetry. This is a result of greater σ than π bonding. Hence, in making the transition $t^6e^2{}^3A_{2g} - t^5e^3{}^3T_{2g}$, there is a decrease in the charge assigned to the metal-ion $3d$ orbitals, which amounts to between 0.025 and 0.037 electrons.

IV. WHAT IS $10Dq$?

It has been a major goal of all previous theoretical studies of transition-metal compounds to calculate the spectral splitting parameter $10Dq$. For NiF_6^{-4} , $10Dq$ may be defined as the energy difference between N -electron states

$$10Dq = E({}^3T_{2g}) - E({}^3A_{2g}) \quad (4.1)$$

Thus we have obtained this quantity in Table V from solutions of the appropriate SCF equations.

A. Contributions to $10Dq$

The many-electron approach of Eq. (4.1) is not in the spirit of semiempirical ligand field theory, which views $10Dq$ as an orbital energy difference. Also it offers no conceptual guidelines to the covalency factors contributing to the magnitude of $10Dq$.

To explore this question we present three distinct analyses. The first may be viewed as a sequence of refinements passing from the original crystal-field model to the SCF result. The others are based

TABLE VIII. Gross atomic population analysis (regular overlaps).

Symmetry orbital		${}^3A_{2g}$			${}^3T_{av}$		
		D	DSP	DDSP	D	DSP	DDSP
a_{1g}	$4s$		0.618	0.617		0.620	0.620
	$2s$	2.000	1.953	1.953	2.000	1.953	1.953
	$2p\sigma$	2.000	1.429	1.430	2.000	1.427	1.428
t_{1u}	$4p$		1.359	1.359		1.365	1.365
	$2s$	6.000	5.917	5.915	6.000	5.916	5.914
	$2p\sigma$	6.000	5.265	5.258	6.000	5.268	5.262
	$2p\pi$	6.000	5.459	5.468	6.000	5.452	5.458
e_g	$3d$	2.117	2.070	2.134	3.068	3.038	3.087
	$2s$	3.995	3.995	3.991	3.997	3.998	3.994
	$2p\sigma$	3.888	3.935	3.875	3.935	3.964	3.919
t_{2g}	$3d$	6.000	6.000	6.011	5.014	5.007	5.021
	$2p\pi$	6.000	6.000	5.989	5.986	5.993	5.978
t_{1g}	$2p\pi$	6.000	6.000	6.000	6.000	6.000	6.000
t_{2u}	$2p\pi$	6.000	6.000	6.000	6.000	6.000	6.000
Total	$2s$	11.995	11.865	11.859	11.997	11.867	11.861
Total	$2p\sigma$	11.888	10.629	10.563	11.935	10.659	10.609
Total	$2p\pi$	24.000	23.459	23.457	24.000	23.445	23.436
Total	$3d$	8.117	8.070	8.145	8.082	8.045	8.108

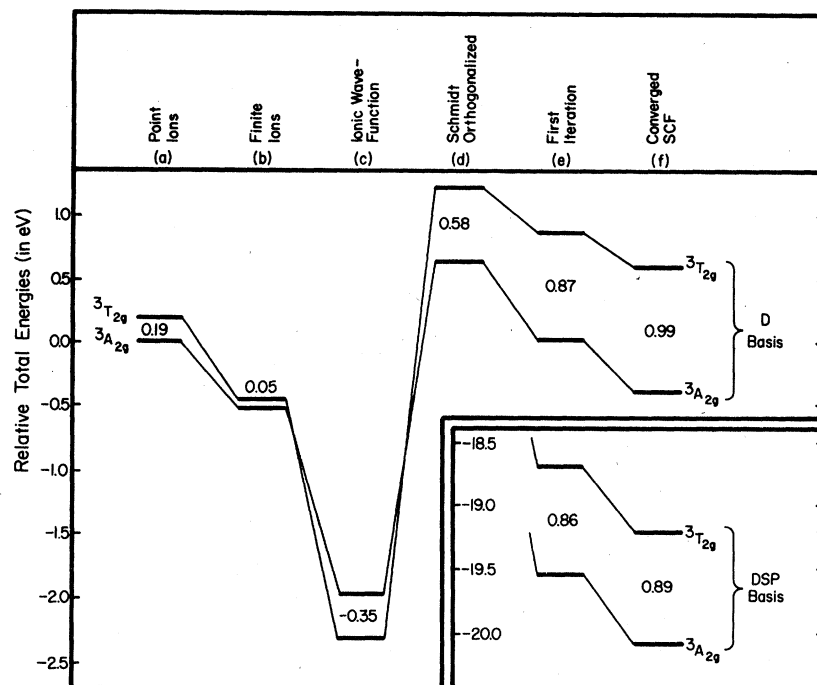


FIG. 1. Energies of the $^3A_{2g}$ and $^3T_{2g}$ states at successive stages of the calculations. Transition energies indicated in the inset refer to the same origin.

upon partitionings of the total transition energy, the second using the same set of SCF MO's for both states, and the third using the two independent SCF results.

Based on the REG and DSP calculations, Fig. 1 displays successive changes in the ground-state total energy and in the transition energy, as follows. At the left, column (a) corresponds to the pure ionic crystal-field model, in which each fluoride ion is assumed to interact as a point charge with the metal and with the other fluorides.³² At column (b) we allow for the actual spacial distribution of the fluoride electrons in evaluating the electrostatic perturbation of the metal by the fluorides (Kleiner's correction³³); there is a substantial reduction in $10Dq$ even from the too small value at column (a), although here the value remains positive. Retaining a formally ionic structure but incorporating the exchange interactions between metal and ligands leads to a sizable lowering of total energies and to an inversion of the levels at column (c). This situation arises because there is a greater number of the larger exchange interactions with the $3de_g$ orbitals in the excited state. One unsatisfactory feature of column (c) is that the metal and ligand orbitals are not mutually orthogonal. Schmidt orthogonalizing the $3d$ AO's to the appropriate ligand symmetry-adapted functions and evaluating the expectation value of the Hamiltonian over $^3A_{2g}$ and $^3T_{2g}$ wave functions constructed from these functions leads to column (d). The orthogonality constraint raises the total energy of $^3T_{2g}$ by more than $^3A_{2g}$, and restores them to proper order. Again this effect arises because

of the greater (overlap) interaction of the $3de_g$ AO's with the ligand orbitals. Orthogonality alone thus yields a transition energy more than half the experimental value.³⁴

Based upon the Schmidt-orthogonalized LCAO coefficients just described, the first iteration of the SCF process may be carried out. From the wave function constructed using these LCAO coefficients, the energies at column (e) may be calculated. Comparatively little net stabilization is found from $3d$ bonding alone. The large decrease in total energy comes from the added participation of the $4s$ and $4p$ orbitals. (See Fig. 1, inset.) These orbitals have very little effect on the computed optical transition energies however. Significantly, the transition energy $10Dq$ has risen to near the experimental value with the final SCF results shown at column (f). We have arrived at the same conclusion as Sugano and Shulman⁴ reached earlier, namely, that the major contributions to $10Dq$ must arise from factors identified with covalency. [Our results column (e), however, should not be directly compared with theirs since, among other things, they used a one-electron Hamiltonian constructed from strictly ionic (nonorthogonalized) orbitals.]

The other partitionings investigated here are based upon separating the *finally* computed transition energy ΔE according to

$$\begin{aligned}\Delta E &= E(^3T_{2g}) - E(^3A_{2g}) \\ &= \Delta H' + \Delta G\end{aligned}\quad (4.2)$$

TABLE IX. Values of the ten independent $t_{2g} - e_g$ electronic repulsion integrals (a.u.).

Integral	Free ion	${}^3A_{2g}$	${}^1T_{av}$	REG D	REG DSP	REG DDSP	${}^3T_{av}$	MOD DSP	3CEN D	3CEN DSP
		REG D	REG D				MOD D			
$\bar{J}(tt)$	0.98788	0.95447	0.96833	0.97292	0.98215	0.95821	0.97126	0.98031	0.97174	0.98085
$\bar{K}(tt)$	0.37458	0.36137	0.36695	0.36875	0.37234	0.36305	0.36810	0.37165	0.36829	0.37186
$K(tt)$	0.04076	0.03889	0.03976	0.04000	0.04049	0.03928	0.03991	0.04039	0.03994	0.04042
$\bar{J}(et)$	0.97287	0.93299	0.92220	0.93627	0.95847	0.93934	0.93559	0.95598	0.93402	0.95641
$\bar{K}(et)$	0.03468	0.03281	0.03237	0.03305	0.03411	0.03321	0.03301	0.03399	0.03294	0.03401
$J(et)$	0.94855	0.90967	0.89914	0.91287	0.93451	0.91585	0.91220	0.93208	0.91067	0.93250
$K(et)$	0.04684	0.04432	0.04372	0.04464	0.04607	0.04486	0.04459	0.04591	0.04449	0.04593
$\bar{J}(ee)$	0.99539	0.94752	0.91288	0.93634	0.97198	0.95701	0.93653	0.96873	0.93301	0.96909
$\bar{K}(ee)$	0.54453	0.51806	0.49889	0.51108	0.53164	0.52332	0.51198	0.52984	0.51002	0.53003
i	0.01053	0.01001	0.01005	0.01019	0.01041	0.01012	0.01017	0.01038	0.01016	0.01039

and serve also to illustrate the methodology for computing transition energies from one given SCF result. $\Delta H'$ will be the net transition energy minus changes in interelectronic Coulomb and exchange energies whose further definition depends upon the adopted scheme of interpretation.

In pure crystal-field theory, which assumes that the transition involves changes only in the occupations of otherwise fixed $3d$ atomic orbitals, $\Delta G \equiv 0$ and $\Delta H' \equiv 10Dq$ for this case.

In the more general theory, however, the transition occurs between the $2t_{2g}$ and $3e_g$ antibonding MO's, which have different radial behavior. The latter are considerably more delocalized and hence the total electrostatic interaction among these largely $3d$ MO's will be lessened in the excited state. This is indicated in Table IX, from which one may observe the greater reduction from free-ion values in integrals involving the $3e_g$ MO. The Coulomb J integrals are very large (~ 27 eV) and even small changes in them are significant compared to $10Dq$.

These ideas may be examined in the second scheme of analysis, in which a fixed set of MO's is selected. From Eq. (2.8) the orbital energies calculated for a given state are

$$\epsilon(i\Gamma) = \underline{C}^\dagger(i\Gamma)\underline{F}(\Gamma)\underline{C}(i\Gamma). \quad (4.3)$$

At convergence the coupling operators \underline{R}_c and \underline{R}_o give zero contribution, and specifically (with $2t_{2g} = t$ and $3e_g = e$),

$$\begin{aligned} \epsilon_0(t) = & H'(t) + [2\alpha_1 \bar{J}(tt) + 2\beta_1 \bar{K}(tt) + 2\gamma_1 K(tt) + \alpha_2 \bar{J}(et) \\ & + \beta_2 \bar{K}(et) + \gamma_2 \bar{J}(et) + \delta_2 K(et)]/n(t), \\ \epsilon_0(e) = & H'(e) + [\alpha_2 \bar{J}(et) + \beta_2 \bar{K}(et) + \gamma_2 J(et) + \delta_2 K(et) \\ & + 2\alpha_3 \bar{J}(ee) + 2\beta_3 \bar{K}(ee)]/n(e). \end{aligned} \quad (4.4)$$

From these equations the $H'(i\Gamma)$ may be calculated

as the sum of kinetic energy, core attraction energy, and Coulomb plus exchange interaction with all orbitals *except* $3e_g$ and $2t_{2g}$; for the specified configuration and state, the α , β , γ , δ coefficients are obtained from Table III.

Now define $\Delta H' = H'(e) - H'(t)$. Then, neglecting configuration interaction, ΔE for the transition

$$t^x e^y {}^S \Gamma - t^{x-n} e^{y+n} {}^{S'} \Gamma'$$

is given by

$$\Delta E = n\Delta H' + G(x-n, y+n; S'\Gamma') - G(x, y; S\Gamma). \quad (4.5)$$

Using Eq. (2.3), Table III, and (for reasons already mentioned for discussion in Sec. V) results from the REG ${}^3T_{av}$ SCF solution, we obtain for the $t^6 e^2 {}^3A_{2g} \rightarrow t^5 e^3 {}^3T_{2g}$ transition

$$\begin{aligned} \Delta G = & -6\bar{J}(tt) + 3\bar{K}(tt) + 2\bar{J}(et) - \bar{K}(et) + J(et) \\ & - K(et) + 2\bar{J}(ee). \end{aligned} \quad (4.6)$$

The first two rows of Table X exhibit values of $\Delta H'$ and ΔG using this "frozen-orbital" method implicit in Eqs. (4.4)–(4.6). In this way we computed $10Dq$ and other spectral transition energies given in Table VI.

At this point, $\Delta H'$ may be viewed as the transition energy in the field of the ligand ions plus the metal-ion core – a conceptual analog of the pure crystal-field $10Dq$ parameter which, however, is seen to be several times larger. The compensating ΔG , as has previously been noted, brings the total ΔE to very nearly the same value for all three bases.

In this frozen-orbital method, not all the change in interelectronic repulsion occurs in ΔG . That part involving interaction of $2t_{2g}$ and $3e_g$ with the other (frozen) valence shell MO's (call it $\Delta G_{v,et}$) may be transferred from $\Delta H'$ to ΔG . For purposes of comparison with the third method of analysis, we also give in the Table X computed values of

TABLE X. Partitionings of ${}^3A_{2g} \rightarrow {}^3T_{2g}$ transition energies, ΔE (in eV).

Partitioning method		D	Basis DSP	DDSP
Frozen orbitals	ΔG	-4.09	-1.65	-0.81
Eqs. (4.2) and (4.5)	$\Delta H'$	5.08	2.54	1.81
	ΔE	0.98	0.89	1.00
Frozen orbitals	$\Delta G''$	-2.81	-0.41	0.56
Eqs. (4.7) and (4.8)	$\Delta H''$	3.80	1.30	0.44
	ΔE	0.98	0.89	1.00
Difference of independent SCF's ^a	ΔG	-0.68	0.21	0.16
	$\Delta H'$	1.67	0.68	0.86
	ΔE	0.99	0.89	1.02

^a ΔG and $\Delta H'$ are changes in total two-electron energies and total kinetic plus core-attraction energies, respectively.

$$\begin{aligned}\Delta H'' &= \Delta H' - \Delta G_{v,et} \\ &= \Delta(T + V)\end{aligned}\quad (4.7)$$

and

$$\Delta G'' = \Delta G + \Delta G_{v,et}, \quad (4.8)$$

where $\Delta(T + V)$ arises only from the difference in kinetic plus core-attraction energies of the $3e_g$ and $2t_{2g}$ MO's, and $\Delta G''$ is the *total* change in two-electron energy.

In the third partitioning method, which is relevant to the "best" transition energies of Table V, we may define the $\Delta H'$ and ΔG of Eq. (4.2) in a manner conceptually paralleling Eqs. (4.7) and (4.8), *except* that the two respective quantities are defined as changes in the total kinetic plus core-attraction energies and in total two-electron energies, calculated in passing between the independently computed ${}^3A_{2g}$ and ${}^3T_{2g}$ states. That is, the frozen-orbital approximation is abandoned. The problems with the $1t_{2g}$ and $2t_{2g}$ MO's previously noted in the ${}^3A_{2g}$ ground state are irrelevant here, since the *total* energy quantities employed here are invariant to any unitary transformation among any occupied MO's.

The results in Table X vividly display the power of the variational method in achieving differences in *total* energy which are much less sensitive than their individual ingredients to changes in basis. They also demonstrate the relatively large degree to which those ingredients may be changed by the additional reorganization of density permitted by doing the independent SCF calculations, even though the net effect on their sum is small.

It is remarkable that, as the calculational methods go further from the philosophy of the original crystal-field theory, the $\Delta H'$ and ΔG values created come closer to its expectations.

B. One-Electron Hamiltonians

It would be convenient to define a one-electron operator, \mathcal{H}_{eff} , such that

$$\begin{aligned}10Dq &= \epsilon(3e_g) - \epsilon(2t_{2g}) \\ &= \underline{C}^\dagger(3e_g)\mathcal{H}_{eff}\underline{C}(3e_g) - \underline{C}^\dagger(2t_{2g})\mathcal{H}_{eff}\underline{C}(2t_{2g}).\end{aligned}\quad (4.9)$$

Formally, this is easily done if, following Sugano and Shulman,⁴ \mathcal{H}_{eff} is Fock-type operator appropriate to the \downarrow spin $2t_{2g}$ MO spin in the ground state or the $3e_g$ MO of \uparrow spin in the excited state.⁷ The ambiguity in using an equation such as (4.9) arises from the question of what one-electron operator should be used to determine the covalency coefficients in the eigenvectors $\underline{C}(3e_g)$ and $\underline{C}(2t_{2g})$.

Certain requirements must be met. The one-electron operators should be those arising from optimizing a proper N -electron MO wave function. Sugano and Shulman used the operator \mathcal{H}_{eff} of Eq. (4.9) also to determine these coefficients. This, however, is not the operator arising in the Hartree-Fock equations for either the ground or the excited state. As pointed out by Sugano and Tanabe,⁷ it lacks the effects of the coupling operators R .

In addition, even if the vector coefficients are determined from some suitable set of eigenvalue equations, their character may significantly change in passing from ground to excited state. In this event, Eq. (4.9) no longer is valid.

We have already seen in Table VII that, unlike the e_g MO's, the closed-shell t_{2g} MO's from the ground-state SCF (especially D and DSP) are much different from those from the $t^5e^3{}^3T_{av}$ SCF and all yield a poor estimate of the spectrum. On the other hand, all properties of the ground-state wave function are invariant to a unitary transformation of the occupied MO's, in particular, one which brings them (as close as possible, depending upon the basis) to the form appropriate to the excited state. We simply observe that in these systems the $t^5e^3{}^3T_{av}$ SCF gives a satisfactory form. Offenhartz³⁵ has proposed using a more general averaged excited state. (Note that the reorganization energies recorded in the first line of Table VI must arise only from alterations in other than t_{2g} MO's.)

Watson and Freeman⁵ and Šimánek and Šroubek⁶ (WFSS) determined the set of covalency parameters for the \downarrow spin $2t_{2g}$ and $3e_g$ orbitals from their orthogonality to the occupied \downarrow spin bonding orbitals whose antibonding counterparts were empty. Because this approach depended on being able to compute the covalency parameters for the vacant antibonding orbital from its orthogonality to the bonding orbitals, it was limited to a treatment of the minimal basis. $10Dq$ obtained from Eq. (4.9) was in poor agreement with experiment, and as remarked

by Offenhartz,³⁵ "10Dq is obtained as a difference in the orbital energy of unoccupied orbitals, a somewhat peculiar point of view physically speaking."

One may readily discover how the difference in character of solutions to closed- and open-shell operators arises, by analyzing the approximate expressions for ionic Fock-matrix elements given by

$$\begin{aligned}\langle \lambda_{3d} | \underline{F}^0 | \lambda_{3d} \rangle &\approx \epsilon^0(3d) + \langle \lambda_{3d} | V_L | \lambda_{3d} \rangle, \\ \langle \lambda_{3d} | \underline{F}^0 | \lambda_L \rangle &\approx \epsilon^0(3d) \langle \lambda_{3d} | \lambda_L \rangle + \sum \langle \lambda_{3d} | V_{L'} | \lambda_L \rangle, \\ \langle \lambda_L | \underline{F}^0 | \lambda_L \rangle &\approx \epsilon^0(L) + \langle \lambda_L | V_M | \lambda_L \rangle + \sum \langle \lambda_L | V_{L'} | \lambda_L \rangle.\end{aligned}\quad (4.10)$$

$\epsilon^0(3d)$ and $\epsilon^0(L)$ are appropriate free-ion 3d and ligand orbital energies, respectively. Watson and Freeman⁵ point out that there are several distinct 3d orbital energies to be considered:

$$\begin{aligned}\epsilon^0(\uparrow 3dt) &= U + 7A - 14B + 5C = -1.414, \\ \epsilon^0(\uparrow 3dt) &= U + 7A - 10B + 7C = -1.275, \\ \epsilon^0(\uparrow 3de) &= U + 7A - 14B + 3C = -1.503, \\ \epsilon^0(\uparrow 3de) &= U + 8A - 6B + 7C = -0.381,\end{aligned}$$

where U contains the kinetic energy and core interaction and A , B , and C are the Racah parameters for the 3d interactions. Numerical values are in a.u. The last orbital energy is that of a virtual or unoccupied orbital. It differs markedly from those for the occupied orbitals by the Coulombic-type interaction integral $A \approx 1$ a.u. which is four times larger than any other valence-shell Coulombic interaction. Watson and Freeman used this orbital energy appropriate to the operator properly describing the closed-shell bonding MO's, each of which is repelled by eight d electrons.

By contrast, the 3d orbital energies appropriate to their Fock matrices for the occupied 3d orbitals depend on the electronic state of the cluster and typically are given by

$$\epsilon^0(3de, t) = U + 7A + \beta B + \gamma C, \quad (4.11)$$

where β and γ are small numbers. Here, the large

3d self-interaction always cancels, giving 7A instead of 8A, roughly corresponding to the motion of one 3d electron in the field of the other seven.

Based upon the Hartree-Fock-Roothaan procedure, Eqs. (2.8), we show typical converged values of the e_g and t_{2g} matrix elements of \underline{F}_o , \underline{F}_c , $(\underline{F}_o + \underline{R}_c)$, and $(\underline{F}_c + \underline{R}_o)$ in Table XI.

Expected properties are clearly evident in the $t^5 e^3 {}^3T_{av}$ diagonal elements of $(\underline{F}_c + \underline{R}_o)$ and $(\underline{F}_o + \underline{R}_c)$ which occur in the secular equations determining the closed- and open-shell eigenvectors, respectively. The $3d^2$ elements of $(\underline{F}_c + \underline{R}_o)$, which weight the participation of the 3d functions in the closed-shell MO's, are much more positive than in $\underline{F}_o + \underline{R}_c$ and "encourage" the closed-shell MO's to remain localized on the ligands. The converse is true for the open-shell MO's. Also evident from these elements is the fact that the same argument which differentiates the open- and closed-shell $3d^2$ elements also applies to the $2s^2$ and $2p^2$ elements, though on a reduced scale since the integrals involved are smaller.

For both symmetries the matrix elements of \underline{F}_c and \underline{F}_o from ${}^3A_{2g}$ are very similar to those from ${}^3T_{av}$ for the e_g symmetry. This is to be expected since there is little difference in the gross features of the charge distribution for the two states. See Table VIII. The near equality of the $3dt^2$ and $2p\pi^2$ elements in all the F matrices accounts for the apparent extreme covalency in t_{2g} MO's of the ${}^3A_{2g}$ state. This near degeneracy is thoroughly lifted by the coupling operators in ${}^3T_{av}$, providing the spectroscopically satisfactory form of the $2t_{2g}$ orbitals.

Because of its pertinence to semiempirical studies and its further exposition of the bonding factors exhibited during convergence during the SCF process, we present an MO correlation diagram in Fig. 2. The figure is based upon the REG D ${}^3T_{av}$ SCF calculation. Energy quantities correlating with the $3e_g$ and $2t_{2g}$ MO's are taken from the open-shell equations; others are from the closed-shell equations.

TABLE XI. Fock matrix elements (in a.u.) with and without the coupling matrix elements, from the converged ${}^3A_{2g}$ and ${}^3T_{av}$ SCF cases (REG DSP calculations).

Matrix element	F_c	$t^6 e^2 {}^3A_{2g}$ F_o	$F_c + R_o$	$F_o + R_c$	F_c	$t^5 e^3 {}^3T_{av}$ F_o	$F_c + R_o$	$F_o + R_c$
$e_g: 3de^2$	0.8535	0.3252	1.8783	0.3890	0.6234	0.3776	2.0090	0.4962
$3de2s$	-0.0806	-0.0795	-0.0934	-0.0583	-0.0800	-0.0921	-0.0985	0.0292
$2s^2$	-0.5073	-0.5088	-0.5073	-0.5032	-0.5062	-0.5946	-0.5062	0.1117
$3de2p\sigma$	-0.0694	-0.0589	-0.1533	0.0672	-0.0643	-0.0819	-0.1865	0.2215
$2s2p\sigma$	0.0164	0.0150	0.0169	0.0200	0.0168	0.0026	0.0169	0.1088
$2p\sigma^2$	0.4839	0.4782	0.4872	0.4947	0.4835	0.3928	0.4890	1.1109
$t_{2g}: 3dt^2$	0.4206	...	0.4206	...	0.5700	0.4067	2.1866	0.4249
$3dt2p\pi$	-0.0281	...	-0.0281	...	-0.0300	-0.0337	-0.0910	0.0843
$2p\pi^2$	0.4674	...	0.4674	...	0.4691	0.4173	0.4703	1.0375

TABLE XII. Unrestricted Hartree-Fock MO coefficients and orbital energies for the ground state of NiF_6^{4-} (REG DDSP).

MO	Symmetry-orbital coefficients					ϵ (in a.u.)	
	$nl(\text{Ni})$	$3d_i(\text{Ni})$	$2s(\text{F})$	$2p\sigma(\text{F})$	$2p\pi(\text{F})$	This work	Ref. 6
α spins:							
$1a_{1g}$	0.0492		0.9758	-0.0209		-0.51136	-0.276
$2a_{1g}$	0.4642		-0.2314	0.7783		0.35493	1.052
$1t_{1u}$	0.0269		0.9858	-0.0111	-0.0016	-0.51282	-0.182
$2t_{1u}$	0.3972		-0.2119	0.5681	0.6157	0.39089	0.814
$3t_{1u}$	0.0438		-0.0171	0.7119	-0.7006	0.46458	1.384
$1e_g$	0.0503	-0.0084	0.9947	-0.0162		-0.51331	-1.023
$2e_g$	0.9217	-0.0285	-0.1134	0.3639		0.25759	0.296
$3e_g$	-0.3988	-0.0710	0.0645	0.9295		0.52789	0.819
$1t_{2g}$	0.9766	-0.0467			0.3137	0.33421	0.392
$2t_{2g}$	-0.3317	-0.0277			0.9488	0.48177	0.792
$1t_{1g}$					1.0000	0.45792	0.697
$1t_{2u}$					1.0000	0.45877	0.832
β spins:							
$1a_{1g}$	0.0506		0.9750	-0.0251		-0.50688	-0.272
$2a_{1g}$	0.4742		-0.2336	0.7718		0.36455	1.064
$1t_{1u}$	0.0287		0.9848	-0.0158	-0.0016	-0.50796	-0.178
$2t_{1u}$	0.4000		-0.2120	0.5095	0.6644	0.39582	0.820
$3t_{1u}$	0.0883		-0.0374	0.7468	-0.6573	0.47492	1.393
$1e_g$	0.0330	-0.0124	0.9968	-0.0209		-0.50793	-1.018
$2e_g$	0.2660	-0.1068	-0.0094	0.9578		0.46574	0.671
$1t_{2g}$	0.8856	-0.0734			0.5336	0.39294	0.455
$2t_{2g}$	-0.5730	0.0006			0.8450	0.49886	0.801
$1t_{1g}$					1.0000	0.45916	0.700
$1t_{2u}$					1.0000	0.46003	0.834

perpendicular to a bond axis can be formally written as

$$\begin{aligned} A' &= A_z^N = 2A_D + A_s + 2(A_\sigma - A_\tau), \\ B' &= A_y^N = -A_D + A_s - (A_\sigma - A_\tau), \end{aligned} \quad (6.2)$$

where $A_D = 2g\mu_B\gamma\mu_N/(5R_L^3)$ is the classical dipolar interaction with the magnetic ion. A_s is the Fermi contact interaction with the ligand nucleus

$$A_s = g\mu_B\gamma\mu_N \left(\frac{8}{3}\pi\right) \sum_{r,s} \rho_{sr}^* \langle \lambda_s | \delta(\vec{R}_L) | \lambda_r \rangle, \quad (6.3)$$

and $A_\sigma - A_\tau$ is the anisotropic dipolar interaction between the electronic and nuclear spins

$$A_\sigma - A_\tau = g\mu_B\gamma\mu_N \sum_{r,s} \rho_{sr}^* \langle \lambda_s | R_L^{-3} P_2(\cos\theta_\sigma) | \lambda_r \rangle - A_D, \quad (6.4)$$

where the ρ_{sr} are elements of the spin-density matrix

$$\rho = \underline{D}_+ - \underline{D}_-. \quad (6.5)$$

The appropriate spin-restricted ligand-field expressions for A_s and A_σ ($A_\tau = 0$) are given by

$$\begin{aligned} A_s &= g\mu_B\gamma\mu_N \left(\frac{8}{3}\pi\right) |\chi_{2s}(\vec{R}_L)|^2 f_s, \\ A_\sigma &= g\mu_B\gamma\mu_N \left(\frac{8}{3}\pi\right) \langle \chi_{2p} | r_L^{-3} | \chi_{2p} \rangle f_\sigma, \end{aligned} \quad (6.6)$$

where $f_s = \frac{1}{3}C_{2s}^2$ and $f_\sigma = \frac{1}{3}C_{2p}^2$, from the $3e_g$ MO. With the values of the integrals taken from Froese's free-ion F^2 functions

$$|\lambda_{2s}(\vec{R}_L)|^2 = 10.726a_0^{-3}$$

and

$$\langle \chi_{2p} | r_L^{-3} | \chi_{2p} \rangle = 6.405 a_0^{-3},$$

TABLE XIII. Significant contributions to the expectation values of the isotropic and anisotropic hyperfine interactions (in a.u.), from the REG DDSP $^3A_{2g}$ MO's.^a

Charge distribution		sr	sp
$\langle \delta(\vec{R}) \rangle$:			
$(2s)^2$	a_{1g}	...	0.0008
	t_{1u}	...	0.0038
$(3d)(2s)$	e_g	0.0398	0.0422
	e_g	0.0020	0.0020
$\langle r_L^{-3} P_2(\cos\theta_\sigma) \rangle$:			
$(4s)^2$		0.0000	-0.0002
$(4p)^2$		0.0000	-0.0002
$(3d)^2$	total	0.0754	0.0751
$(2p\sigma)^2$	a_{1g}	...	0.0063
	t_{1u}	...	0.0230
$(2p\pi)^2$	e_g	0.0888	0.1000
	t_{1u}	...	0.0032
$(3d)(2p\sigma)$	t_{2g}	0.0000	0.0002
	e_g	-0.0109	-0.0121
$(3d)(2s)$	e_g	-0.0021	-0.0020

^asr means spin-restricted and sp means spin-polarized SCF results. Contributions from $3d$ and $3d_i$ have been combined.

TABLE XIV. Calculated and experimental hyperfine parameters, A_s and $A_0 - A_r$ (10^{-4} cm $^{-1}$), for NiF_6^{4-} .

Case		A_s	$A_0 - A_r$
Spin-restricted	DDSP	29.29	3.144
Spin-polarized	DSP	33.26	3.171
Spin-polarized	DDSP	33.77	4.791
Experiment:			
ESR(KMgF_3) ^a		39.2 ± 0.3	6.9 ± 0.3
NMR(KNiF_3)		33.9 ± 0.4	8.1 ± 1.4
(Ref. 4)			

^aT. P. P. Hall, W. Hayes, R. W. H. Stevenson, and J. Wilkens, *J. Chem. Phys.* **38**, 1977 (1963).

one can use the measurement of the hyperfine parameters to determine the covalency parameters in the open $3e_g$ MO of the ground state. The validity of this approach to determining covalency parameters in the more general SCF wave function is indicated by the magnitude of the other significant contributions to Eqs. (6.3) and (6.4), shown in Table XIII. The largest factor arises from spin polarization.

In Table XIV, we compare the experimental hyperfine interaction parameters to the computed values which were obtained from Eqs. (6.3) and (6.4) using Gauss-Legendre numerical quadrature for the integrals.

The agreement obtained in the case of the isotropic hyperfine interaction must be regarded as fortuitous since the effects involving the ligand $1s$ orbital are not included. In an effort to approximate them, we orthogonalized the metal-ion orbitals to the $1s$ and obtained a large negative correction from the $(\lambda_{3d}^{\text{ortho}})(\lambda_{2s})$ charge distribution, which is similar to that obtained by Marshall and Stuart.³⁷ The problem is difficult because it requires an accurate wave function at the ligand nucleus and is perhaps better approached by the method suggested by Ellis, Freeman, and Ros in looking at clusters of the type $(\text{Ni}_2\text{F}^{+3})$.

Results for $A_0 - A_r$ are in good agreement with experimental values from which orbital moment contributions have been removed; they show strong σ -bonding interaction. A calculation based upon $3d$ AO's which were merely Schmidt orthogonalized to the ligand symmetry-adapted functions gave $A_s = 19.39 \times 10^{-4}$ cm $^{-1}$ and $A_0 - A_r = 0.34 \times 10^{-4}$ cm $^{-1}$. These results indicate that significant electron delocalization, beyond the minimal orthogonality requirement, is needed to explain the magnitude of the observed hyperfine interactions. We also see from Table XIV that expanding the basis to DDSP increases the calculated parameters, in agreement with our observation (see Table VIII) that this most flexible

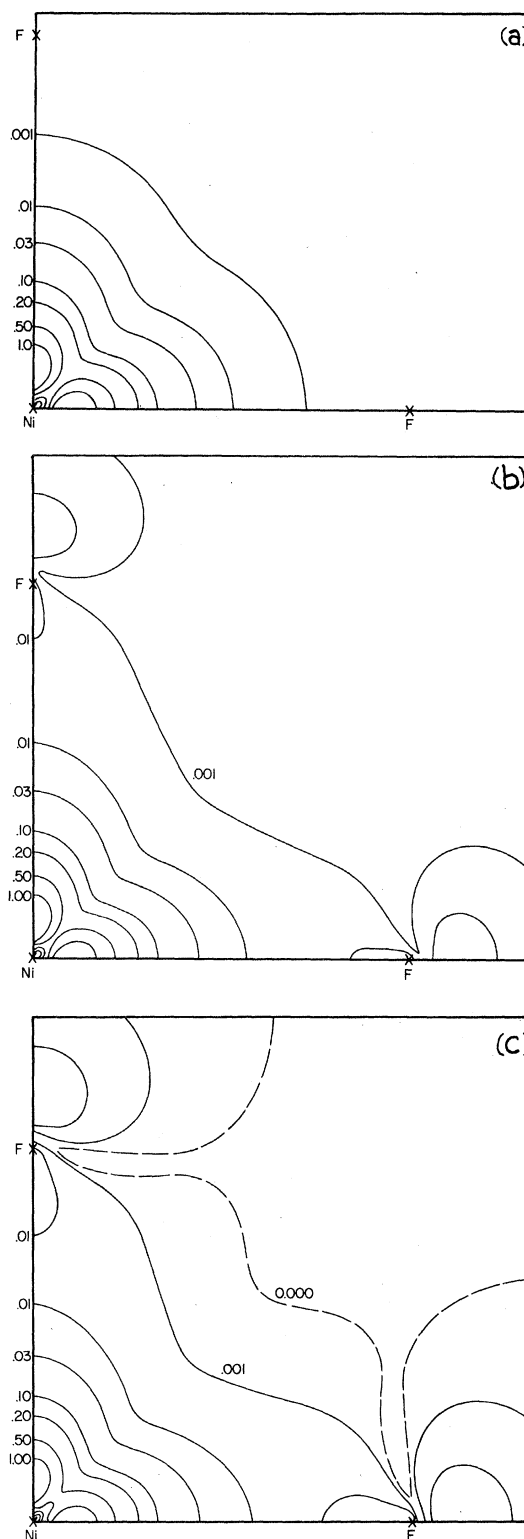


FIG. 3. Ground-state spin-density distribution contours in an F-Ni-F plane, in units of a_0^{-3} : (a) purely ionic structure; (b) spin-restricted SCF results; (c) spin-polarized SCF results. Note that net negative spin density occurs in the upper right region of (c). DDSP REG calculations.

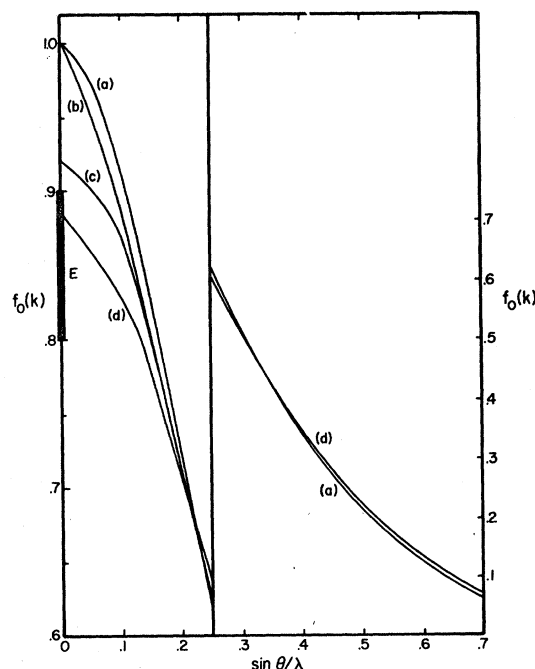


FIG. 4. Spherical components of the neutron magnetic form factor: curve (a), free Ni^{+2} ion; curve (b), free sr NiF_6^{-4} cluster; curve (c), sr NiF_6^{-4} cluster, without ligand-only contributions; curve (d), sp NiF_6^{-4} cluster, without ligand-only contributions; E is range of the experimental absolute forward-scattering factor. Note change of scale at $\sin\theta/\lambda = 0.25$. DDSP REG calculations.

basis leads to the greatest net charge transfer into the $3d$ orbitals.

Spin polarization increases $A_\sigma - A_\pi$ by more than 25%. It has the effect of allowing a greater net \uparrow spin density in the region of σ bonding, as can be seen from the net spin-density distribution function $\rho(\vec{r})$. Figure 3 shows contours of $\rho(\vec{r})$ in a plane through the Ni and two F's, Fig. 3(a) for the spin-restricted ground-state solutions of the free Ni^{+2} ion, Fig. 3(b) for the spin-restricted and Fig. 3(c) for the spin-polarized wave functions for the cluster. Comparing Fig. 3(a) to Fig. 3(b) shows the effect of covalent bonding on the unpaired $3e_g$ orbitals. Comparing to Fig. 3(c) shows the additional contributions from spin polarization, which increases the \uparrow spin density in the region of the $2p\sigma$ ligand orbitals and is also responsible for the net negative or \downarrow spin density in the region of the $2p\pi$ orbitals. This also has important consequences in the calculation of the low-angle neutron scattering factor.

A. Neutron Magnetic Form Factors

Magnetic Bragg-scattering amplitudes are proportional to the Fourier transform of the spin-density distribution within a unit cell

$$f_0(\vec{k}) = \int_{\text{unit cell}} \rho(\vec{r}) e^{i\vec{k}\cdot\vec{r}} d\vec{r}. \quad (6.7)$$

We limit our discussion to the spherically averaged component for which Eq. (6.7) becomes

$$f_0(k) = \int_{\text{unit cell}} \rho(r) j_0(kr) d^3r, \quad (6.8)$$

where $j_0(kr)$ is the zeroth-order Bessel function. The integrals appearing in Eq. (6.8) were evaluated by the same method as used in Eq. (6.4).

Hubbard and Marshall³⁸ studied the effects of covalency on the measured neutron magnetic form factors for ferromagnetic and antiferromagnetic salts using a Heitler-London LCAO wave function. They showed that the forward-scattering amplitude should be reduced by covalent bonding and the form factor raised above that of the free ion. In simple-cubic antiferromagnetic salts, the forward-scattering amplitude $k=0$ measures the magnetic moment integrated over a unit cell containing the magnetic ion. It is slightly reduced because the spin density which is transferred to the region of the neighboring ligand ion between two magnetic ions will be canceled by contributions of opposite sign.

We used the suggestion of Hubbard and Marshall in evaluating the integral appearing in Eq. (6.8) by subtracting the contributions due to ligand-only charge distributions.

Figure 4 displays form factors obtained from various cluster calculations and from the free ion, curve (a). Comparing the spin restricted curves (b) and (c) shows the reduction in forward scattering results from the subtraction of density components associated only with the ligands. Passing from curves (c) to (d) indicates the further reduction in the forward direction produced by spin polarization. Subtracting the consequent greater \uparrow spin density associated with the $2p\sigma$ orbitals leads to the additional flattening of the low-angle portion of the scattering curve. Adding contributions from core polarizations and orbital moments would produce small changes in the large-angle region.³⁸

Comparisons with scaled experimental form factors for NiO have previously been given.³¹ The ligand-corrected forward-scattering factor calculated from the spin-polarized wave function falls within the range recently determined experimentally by Hutchings and Guggenheim, 0.85 ± 0.050 .³⁹

VII. CONCLUDING REMARKS

Encouragingly good agreement with experiment has been obtained for both the optical spectrum and magnetic properties. In contrast to most earlier calculations, we adopted a many-electron point of view and obtained self-consistent solutions for the ground and various excited states of the cluster. The best computed spectrum was obtained from differences in total energy. However, we found that the spectrum could almost as well be computed

from open-shell solutions from a single SCF calculation if that calculation was done for an excited configuration. Such open-shell MO's give good approximations even to the total energy of the ground state.

In these calculations, all three- and four-center integrals have been variously approximated. Most of these multicenter integrals enter into the calculation only in proportion to the extent to which the true wave function differs from a strictly ionic condition. Nevertheless, it is important to evaluate all three- and four-center integrals in order to test the effect of these approximations on the computed spectral transitions. Indications are that these integral approximations are quite good for this sys-

tem and type of basis.¹⁵ Furthermore, the calculated physical properties were not found to be especially sensitive to the extensions of the basis considered.

An alternative description of covalent bonding was given by Hubbard, Rimmer, and Hopgood,⁴⁰ who derived essentially a valence-bond-type wave function as a linear combination of Slater determinants representing the ionic ground and various excited "charge transfer" configurations. We conclude, however, that the open-shell LCAO MO SCF method applied to discrete clusters provides a satisfactory explanation of the low-energy electronic spectrum and the gross magnetic features of nickel fluoride salts.

*Work supported by Contract SD-102 with the Advanced Research Projects Agency. Based in part on the doctoral dissertation of T. F. Soules.

†Present address: Lighting Research Laboratory, General Electric Company, Cleveland, Ohio 44112.

‡Present address: Chemistry Department, Memphis State University, Memphis, Tenn. 38111.

¹P. W. Anderson, *Solid State Phys.* **14**, 99 (1963).

²J. H. Van Vleck, *J. Chem. Phys.* **3**, 803 (1935).

³J. P. Dahl and C. J. Ballhausen, in *Advances in Quantum Chemistry*, Vol. 4, edited by P. O. Löwdin (Academic, New York, 1968).

⁴S. Sugano and R. G. Shulman, *Phys. Rev.* **130**, 517 (1963).

⁵R. E. Watson and A. J. Freeman, *Phys. Rev.* **134**, A1526 (1964).

⁶E. Šimánek and Z. Šroubek, *Phys. Status Solidi* **4**, 251 (1964).

⁷S. Sugano and Y. Tanabe, *J. Phys. Soc. Japan* **20**, 1155 (1965).

⁸P. O'D. Offenhartz, *J. Chem. Phys.* **47**, 2951 (1967).

⁹D. E. Ellis, A. J. Freeman, and P. Ros, *Phys. Rev.* **176**, 688 (1968).

¹⁰In addition to the alternate STO basis here and the one-center basis used in Ref. 9, Gaussian orbital calculations without integral approximation have also been done. See Refs. 11-13.

¹¹H. M. Gladney and A. Veillard, *Phys. Rev.* **180**, 385 (1969).

¹²C. Hollister, J. W. Moscovitz, and H. Basch, *Chem. Phys. Letters* **3**, (1969).

¹³A. J. H. Wachters (private communication).

¹⁴J. W. Richardson, D. M. Vaught, T. F. Soules, and R. R. Powell, *J. Chem. Phys.* **50**, 3633 (1969).

¹⁵J. W. Richardson *et al.* (unpublished).

¹⁶K. Knox, R. G. Shulman, and S. Sugano, *Phys. Rev.* **130**, 512 (1963).

¹⁷J. Ferguson and H. J. Guggenheim, *J. Chem. Phys.* **44**, 1095 (1966).

¹⁸J. Ferguson, H. J. Guggenheim, and D. L. Wood, *J. Chem. Phys.* **40**, 822 (1964).

¹⁹M. Balkanski, P. Moch, and R. G. Shulman, *J. Chem. Phys.* **40**, 1897 (1964).

²⁰J. S. Griffith, *The Theory of Transition Metal Ions* (Cambridge U. P., Cambridge, England, 1964).

²¹C. C. J. Roothaan, *Rev. Mod. Phys.* **23**, 69 (1951).

²²Y. Tanabe and S. Sugano, *J. Phys. Soc. Japan* **9**, 753 (1954).

²³C. C. J. Roothaan, *Rev. Mod. Phys.* **32**, 179 (1960).

²⁴C. C. J. Roothaan and P. S. Bagus, *Methods in Computational Physics* (Academic, New York, 1963), Vol. 2, pp. 47-94.

²⁵See, for example, the review article by G. Berthier, in *Molecular Orbitals in Chemistry, Physics and Biology*, edited by P. O. Löwdin and B. Pullman (Academic, New York, 1964), pp. 57-82.

²⁶J. W. Richardson, W. C. Nieuwpoort, R. R. Powell, and W. F. Edgell, *J. Chem. Phys.* **36**, 1057 (1962); J. W. Richardson, R. R. Powell, and W. C. Nieuwpoort, *ibid.* **38**, 796 (1963).

²⁷R. S. Mulliken, *J. Chim. Phys.* **46**, 497 (1949).

²⁸C. J. Ballhausen, *Ligand Field Theory* (McGraw-Hill, New York, 1962).

²⁹R. G. Shulman and K. Knox, *Phys. Rev. Letters* **4**, 603 (1960).

³⁰A. J. Freeman and D. E. Ellis, *Phys. Rev. Letters* **24**, 516 (1970).

³¹T. F. Soules and J. W. Richardson, *Phys. Rev. Letters* **25**, 110 (1970).

³²Compare A. J. Freeman and R. E. Watson, *Phys. Rev.* **120**, 1254 (1960).

³³W. H. Kleiner, *J. Chem. Phys.* **20**, 1784 (1952).

³⁴Compare Y. Tanabe and S. Sugano, *J. Phys. Soc. Japan* **11**, 864 (1956).

³⁵P. O'D. Offenhartz, *J. Am. Chem. Soc.* **91**, 5699 (1969).

³⁶R. E. Watson and A. J. Freeman, *Phys. Rev.* **123**, 2027 (1971).

³⁷W. Marshall and R. Stuart, *Phys. Rev.* **123**, 2048 (1961).

³⁸J. Hubbard and W. Marshall, *Proc. Phys. Soc. (London)* **86**, 561 (1965).

³⁹M. T. Hutchings and H. J. Guggenheim, *J. Phys. C* **3**, 1303 (1970).

⁴⁰J. Hubbard, D. E. Rimmer, and F. R. A. Hopgood, *Proc. Phys. Soc. (London)* **88**, 13 (1966).